High Performance InGaAs/GaAs Quantum Well Infrared Photodetectors

S. D. Gunapala

Center for Space Microelectronics Technology, Jet Propulsion Laboratory, California Institute of Technology, PasadenaCA91109

K. M. S. V. Bandara[a], B. F. Levine

AT&T Bell Laboratories, Murray Hill, NJ 07974

J. S. Park, T. L. Lin, W. T. Pike, and J. K. Liu

Center for Space Microelectronics Technology, Jet Propulsion Laboratory, California Institute of Technology, Pasadena, CA 91109

ABSTRACT

By increasing the quantum well barrier width, incorporating spacer layers between the contacts and the multi quantum well region, and optimizing the materials growth parameters, we have dramatically reduced the dark current by many orders of magnitude and thereby significantly increased the defectivity. For $In_{0.2}Ga_{0.8}As/GaAs$ quantum well infrared photodetectors having a cutoff wavelength λ_c = 18.3 pm, we have achieved D*= 1.8 x 10^{10} cm$\sqrt{Hz}$/W at temperature T = 40 K.

a) Present address: Department of Physics, University of Peradeniya, Peradeniya, Sri Lanka

There has been much interest in very long-wavelength $GaAs/Al_xGa_{1-x}As$ quantum well infrared photodetectors[1-4] (QWIPs) and associated intersubband absorption (for extensive review see Ref. 5), due to their mature technology and the possibility of producing high performance large area two-dimensional imaging arrays. Due to the possibility of large 2-D arrays and additional advantages such as low I/f noise, low power dissipation, high differential resistance and high radiation hardness these QWIPs should be suitable for very long-wavelength applications such as global temperature monitoring (e.g. earth observing satellites) and long-wavelength astronomy. Since the quality of the barriers is extremely important for optimum QWIP performance, and the fact that binary barrier QWIPs have superior carrier transport properties[6,7], it is interesting to study the $GaAs/In_xGa_{1-x}As$ materials system for very long-wavelength QWIPs. In this letter we discuss *the first high-defectivity* ($D^* = 1.8 \times 10^{10}$ cm$\sqrt{Hz}$/W) $GaAs/In_xGa_{1-x}As$ QWIP in the very long-wavelength infrared region at $\lambda_p = 16.8$ μm (operating at a temperature of T = *40* K),

To achieve this we have grown non-lattice matched $GaAs/In_{0.2}Ga_{0.8}As$ QWIPs via molecular beam epitaxy on a semi-insulating GaAs substrate. Unlike the usual $GaAs/Al_xGa_{1-x}As$ QWIPs, in these structures the heavily doped contacts are made using the high bandgap (i.e. GaAs) semiconductor. As shown in Fig. 1, they consisted of *0.5* μm GaAs top and 1 μm bottom contact layers Si doped with 1×10^{17} cm^{-3} and 10 sets of doped (doping density $N_D = 5 \times 10^{17}$ cm^{-3}) $In_{0.2}Ga_{0.8}As$ quantum wells of well width L_w, separated by nine 600 Å undoped GaAs barriers. In addition, all of these structures consist of two 600 Å thick GaAs spacer layers between the quantum wells and the top and bottom contact layers. It has been previously demonstrated that these spacer layers can significantly reduce the tunneling injection current from contacts to the quantum well region[7] (and hence have a lower dark current). Three samples were grown (in three consecutive days), having L_w = 50 Å, 60 Å and 70 Å. Despite the 1.2% lattice mis-match between $In_{0.2}Ga_{0.8}As$ and GaAs, we were able to grow excellent quality non-lattice matched $GaAs/In_{0.2}Ga_{0.8}As$ QWIP structures as shown in Fig. 2.

The structural parameters of the three samples have been chosen to give a very wide variation in the QWIP absorption and transport properties. Sample A was design to have a intersubband infrared absorption transition Occurnng between a single localized

bound state in the quantum well and a delocalized state in the *continuums.* Sample C , was designed with a wider well width L_w = 70A, yielding two *bound* states in the well. Therefore, the intersubband transition is from the *bound* ground state to the *bound* excited state[10,11] and requires electric field assisted tunneling for the photoexcited carrier to escape into the continuum[10,11]. Due to the low effective mass of the electrons in the GaAs barriers, the electric field required for the field assisted tunneling is expected to be smaller in this structures in comparison to the usual $GaAs/Al_xGa_{1-x}As$ QWIP structures. Sample B was designed such that the second bound level is resonant with the conduction band of the GaAs barrier. Thus, the intersubband transition is from the *bound* ground state to the ***quasibound*** excited state which is intermediate between a strongly bound excited state and a weakly bound continuum state. (See the inserts in Fig. 3 for a schematic conduction band diagram of all three types of QWIP structures.)

All of the QWIPs were processed into 200 μm diameter mesas (area = 3.14×10^{-4} cm^2) using wet chemical etching and Au/Ge ohmic contacts were evaporated onto the top attd bottom contact layers. The dark current-voltage curves for all three samples were measured as a function of temperature from T = 20-50 K and Fig. 3 shows the dark current-voltage curves of all three samples at two different temperatures (T = 30 and 50 K). Note that the dark current shown in Fig. 3 decreases with increasing quantum well width L_w. This is due to the fact that the effective barrier height of the ground state electrons ($E_E = \Delta E_C - E_0 - E_F$) increases with the increasing quantum well width L_w, as shown in the inset of Fig. 3. This increase in effective barrier height reduces both tunneling and thermionic emission of ground state electrons into the continuum transport states, resulting in a lower dark current.

The responsivity spectra of these detectors were measured using a 1000 K blackbody source and a grating monochromator. The detectors were back illuminated through a 45" polished facet[5] and their. responsivity spectrums are shown in Fig. 4. The responsivities of samples A, B and C peak at 12.3, 16.0 and 16.7 μm respectively. The absolute peak responsivities (R_p) of the detectors were measured using a calibrated blackbody source and the peak responsivities (R_p) of the samples A, B and C are 293, 510 and 790 mA/W respectively at bias V_B = 300 mV. As can be readily seen in Fig. 4, the responsivity spectra of the *bound-to-continuum* QWIP (sample A) is much broader than the *bound-to-bound* (sample C) or ***bound-to-quasibound*** (sample B) QWIPs.

Correspondingly, the magnitude of the peak absolute responsivity (R_p) is significantly lower than that for the *bound-to-bound* or *bound-to-quasibound* QWIPs, due to the reduction of absorption coefficient α. This reduction in the absorption coefficient is a result of the conservation of oscillator strength[12]. These peak wavelengths and the spectral widths are in good agreement with theoretical "estimates (see Table 1) of *bound-to-continuum* and *bound-to-bound* intersubband transition based on the 55% conduction band offset ($\Delta E_C / E_g$) of GaAs/$In_{0.2}Ga_{0.8}As$ materials system (i.e. $\Delta E_V / E_g$ = 45%). The measured absolute responsivities of all three samples increase nearly linearly with the bias reaching Rp = 0.85, 1.1 and 2.2 A/W at V_B = 1.3 V for the samples A, B and C respectively. The higher responsivity of the sample C [13,14] *(bound-to-bound)* in comparison to the samples A and B *(bound-to-continuum and bound-to-quasibound)* attributes to the higher absorption coefficient of sample C relative to the other samples and the higher tunneling probability associated with the lower effective mass in the GaAs barriers (in comparison to the higher effective mass in the $Al_xGa_{1-x}As$ barriers of *bound-to-bound* GaAs/$Al_xGa_{1-x}As$ QWIPs).

The current noise in was measured using a spectrum analyzer and experimentally determined the optical gain [15] g using $g = i_n^2 / 4eI_D\Delta f + 1/2N$, where Af is the measurement band width and N is the number of quantum wells. As shown in Fig. 5, optical gain of the sample C reached 22.5 at V_B = 800 mV which is very large compared to the optical gains of usual $Al_xGa_{1-x}As$/GaAs QWIPs. Since the gain of QWIP is proportional to the number of quantum wells N, the better comparison would be the well capture probability p_c, which is directly related to the gain [15] by $g = 1/Np_c$. The calculated well capture probabilities are 20% at very low bias (V_B = 10 mV) and 0.4% at high bias voltage (V_B = 800 mV) which indicates the excellent hot-electron transport in this device structures. This may be a result of the high mobility binary GaAs barriers. The peak defectivity D* can now be calculated from $D^* = R\sqrt{A\Delta f}/i_n$, where A is the area of the detector and A = 3.14x 10^{-4} cm^2. Table 1 shows the D* values of all three samples at temperature T =50 K at a bias of V_B = 300 mV. As shown in the Table 2 the defectivity values of these detectors increase with decreasing temperature.

In summary, we have demonstrated the first high-defectivity (D* = 1.8 x 10^{10} cm$\sqrt{Hz}$/W) very long-wavelength (Xc = 18 μm) $In_xGa_{1-x}As$/GaAs QWIP operating at T = 40 K. The large responsivity and defectivity D* values are superior to those

achieved with the usual lattice matched $GaAs/Al_xGa_{1-x}As$ materials system. The high , optical gains and the small carrier capture probabilities demonstrate the excellent carrier transport of the GaAs barriers and the potential of this heterobarrier system for very long-wavelength ($\lambda > 14\ \mu m$) QWIPs. By comparing the theoretically calculated peak wavelengths and spectral widths we have determined the band offsets ΔE_c and ΔE_v for the non-lattice matched $GaAs/In_xGa_{1-x}As$ het~ob~er-

We are grateful to C. A. Kukkonen, V. Sarohia, S. Khanna, K. M. Koliwad, and B. A. Wilson of the Jet Propulsion Laboratory for encouragement and support of this work. The research described in this paper was performed partly by the Center for Space Microelectronics Technology, Jet Propulsion Laboratory, California Institute of Technology, and was jointly sponsored by the Ballistic Missile Defense Organization/Innovative Science and Technology Office, and the National Aeronautics and Space Administration, Office of Advanced Concepts and Technology.

REFERENCES

1. A" Zussman, B. F. Levine, J. M. Kuo, and J. de Jong, J. Appl. Phys. 70, 5101 (1991).
2. B. F. Levine, A Zussman, J. M. Kuo, and J. de Jong, J. Appl. Phys. 71, 5130 (1992).
3. G. Sarusi, B. F. Levine, S. J. Pearton, and R. E. Leibenguth (to be published).
4. G. Sarusi, B. F. Levine, S. J. Pearton, K. M. S. V. Bandara, and R. E. Leibenguth (to be published).
5. B. F. Levine, J. Appl. Phys. 74, R1 (1993).
6. S. D. Gunapala, B. F. Levine, D. Ritter, R. A. Harem, and M. B. Panish, Appl. Phys. Lett. 58,2024 (1991).
7. S. D. Gunapala, K. M. S. V. Bandara, B. F. Levine, G. Sarusi, D. L. Sivco, and A. Y. Cho (to be published).
8. B. F. Levine, C. G. Bethea, G. Hasnain, V, O, Shen, E. Pelve, R. R. Abott, and S. J. Hseih, Appl. Phys. Lett. 56,851 (1990).
9. A. G. Steele, H. C. Liu, M. Buchanan, and Z. R. Wasilewski, Appl. Phys. Lett. 59, 3625 (1991).
10. B. F. Levine, R. J. Malik, J. Walker, K. K. Choi, C. G. Bethea, D. A. Kleinman, and J. M. Vandenberg, Appl. Phys. Lett. 50,273 (1987).
11. K. K. Choi, B. F. Levine, C. G. Bethea, J. Walker, and R. J, Malik, Phys. Rev. Lett. 59,2459 (1987).
12. S. D. Gunapala, B. F. Levine, L. Pfeiffer, and K. West, J. Appl. Phys. 69, 6517 (1990).
13. The first excited state of the sample C is located 20 meV below the conduction band edge of the GaAs barrier. This state can becomes a quasibound state as a result of band bending due to Si dopant migration into the growth direction.
14. C. Y. Lee, M. Z. Tidrow, K. K. Choi, W. H. Chang, and L. F. Eastman (to be published).
15. W. A. Beck (to be published).

TABLE I. Experimental detectivities and experimental and theoretical spectral data of all three samples at temperature T = 50 K.

Samples	Detectivity ($cm\sqrt{Hz}/W$) Bias V_B=0.3V	Peak wavelength (μm) Experimental	Peak wavelength (μm) Theoretical	Spectral width $\Delta\lambda/\lambda$ Experimental	Spectral width $\Delta\lambda/\lambda$ Theoretical
A	2.9×10^8	12.3	12.5	60%	61%
B	1.0×10^9	16.0	16.3	41%	34%
c	3.0×10^9	16.7	16.8	18%	22%

TABLE II. Experimental detectivities of sample C at *various* temperatures.

Temperature (K)	Defectivity ($cm\sqrt{Hz}/W$)
10	1.3×10^{13}
20	5.4×10^{12}
30	2.9×10^{11}
40	1.8×10^{10}
50	3.0×10^{9}

FIGURE CAPTIONS

Fig. 1 Conduction-band diagram of the $In_{0.15}Ga_{0.85}As/GaAs$ QWIP structure.

Fig. 2 Cross-section transmission electron micrograph of $In_xGa_{1-x}As/GaAs$ QWIP structure. Inset shows atomic resolution image taken along <100>.

Fig. 3 Dark current-voltage curves of all three samples at temperatures T = 30 and 50 K. The inset show the schematic conduction band diagram for sample A (*bound-to-continuum),* sample B (*bound-to-quasibound*), and sample C *(bound-to-bound)).*

Fig. 4 Responsivity spectrums of samples A, B, and Cat temperature T = 50 K. The peak responsivities are R_p = 293,510, and 790 mA/W (at V_B = 300 mV) for samples A, B, and C respectively.

Fig. 5 Optical gain versus bias voltage for sample C device structures at temperature T = 40 K.

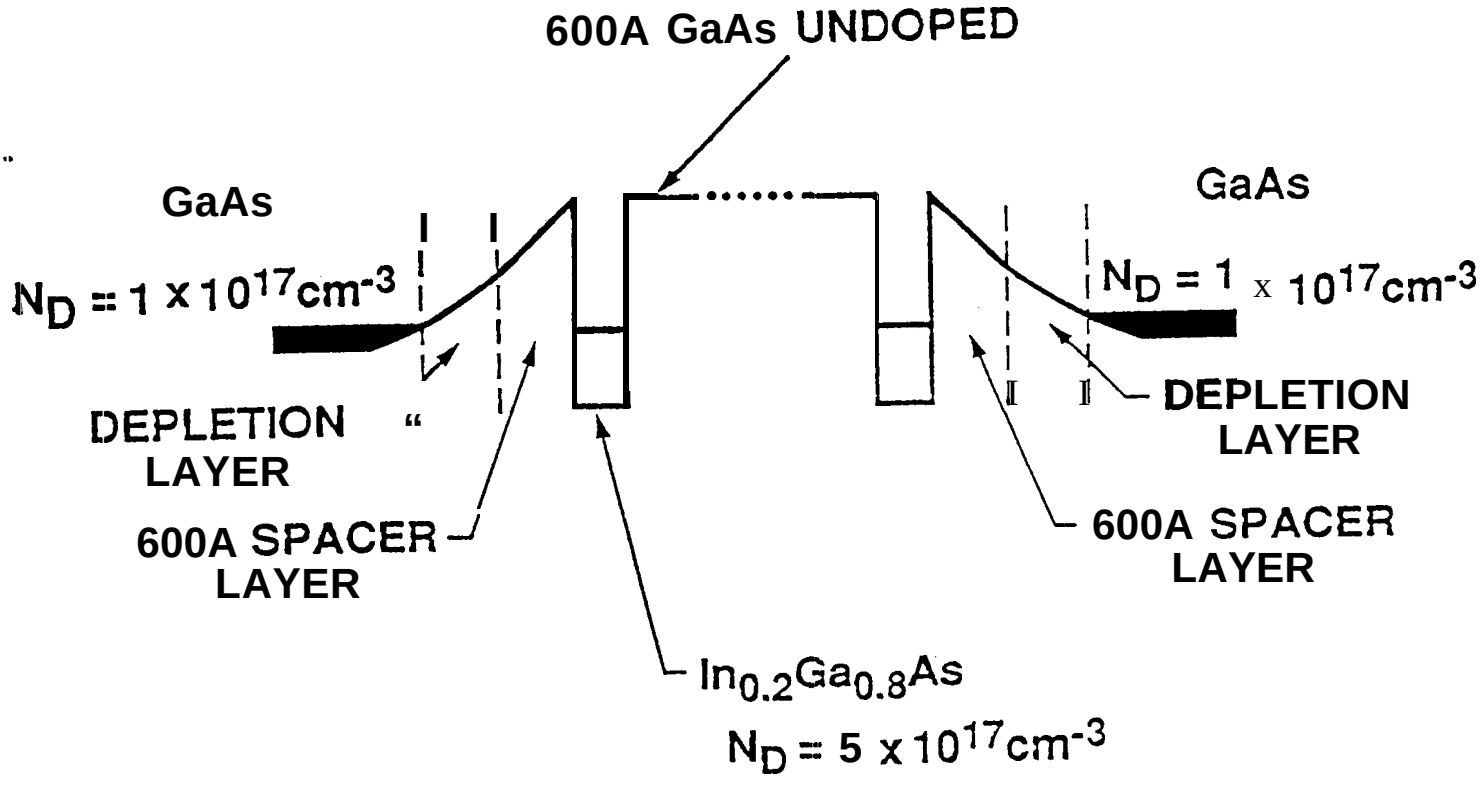
600A GaAs UNDOPED
GaAs
$N_D = 1 \times 10^{17} cm^{-3}$
GaAs
$N_D = 1 \times 10^{17} cm^{-3}$
DEPLETION LAYER
DEPLETION LAYER
600A SPACER LAYER
600A SPACER LAYER
$In_{0.2}Ga_{0.8}As$
$N_D = 5 \times 10^{17} cm^{-3}$

FIG

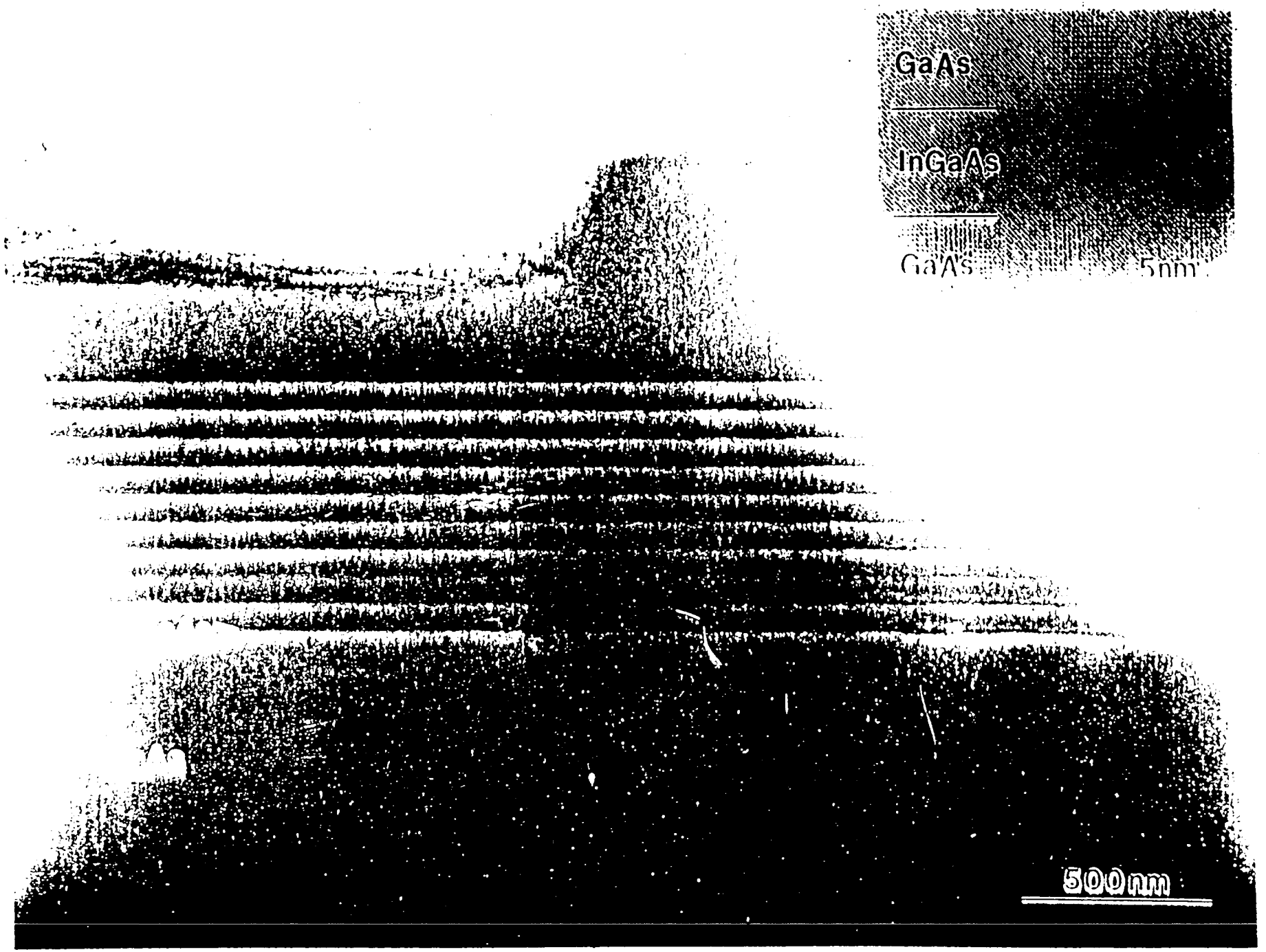
GaAs
InGaAs
GaAs
5nm
500nm

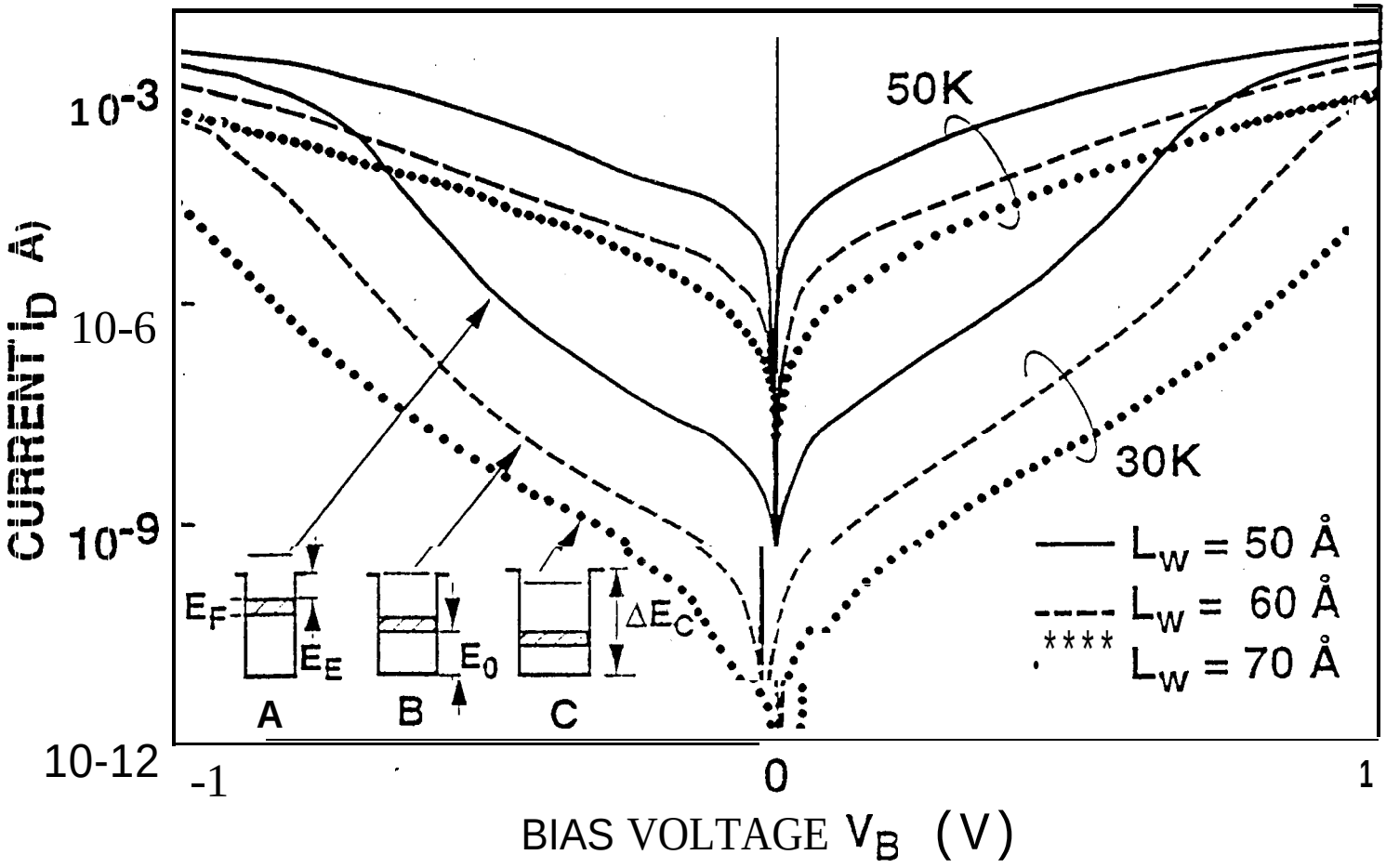
CURRENT i_D (A)
10^{-3}
10-6
10^{-9}
10-12
-1
0
1
BIAS VOLTAGE V_B (V)
50K
30K
L_W = 50 Å
L_W = 60 Å
L_W = 70 Å
E_F
E_E
E_0
ΔE_C
A
B
C

FIG 3

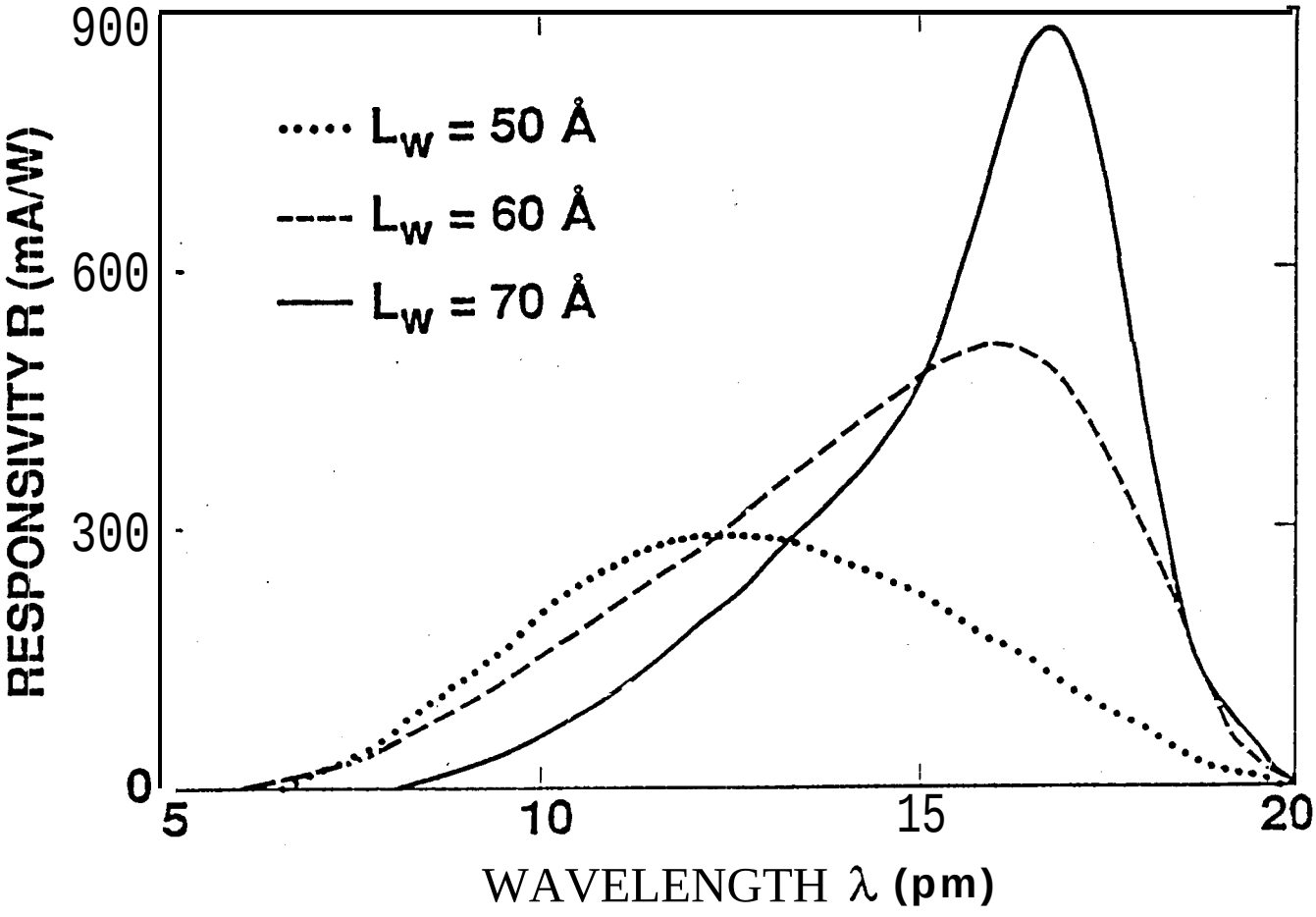
900
600
300
0
RESPONSIVITY R (mA/W)
L_W = 50 Å
L_W = 60 Å
L_W = 70 Å
5
10
15
20
WAVELENGTH λ (pm)

FIG.

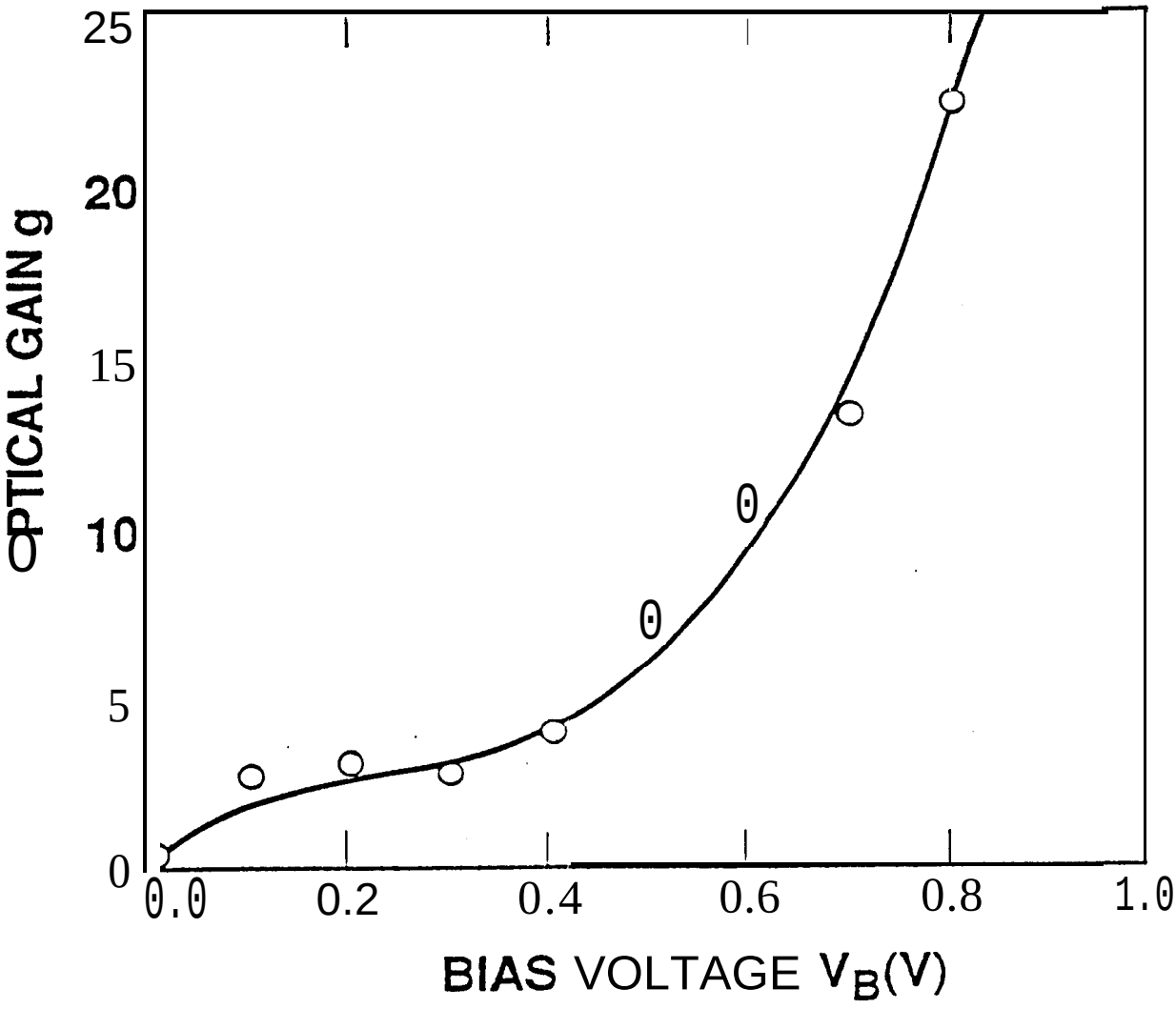

FIG. 5